Organic Chemistry

DOI: 10.1002/anie.201309585

Potential-Driven Chirality Manifestations and Impressive Enantioselectivity by Inherently Chiral Electroactive Organic Films**

Francesco Sannicolò, Serena Arnaboldi, Tiziana Benincori, Valentina Bonometti, Roberto Cirilli, Lothar Dunsch, Włodzimierz Kutner, Giovanna Longhi, Patrizia R. Mussini, Monica Panigati, Marco Pierini, and Simona Rizzo*

Abstract: *The typical design of chiral electroactive materials involves attaching chiral pendants to an electroactive polyconjugated backbone and generally results in modest chirality manifestations. Discussed herein are electroactive chiral polyheterocycles, where chirality is not external to the electroactive backbone but inherent to it, and results from a torsion generated by the periodic presence of atropisomeric, conjugatively active biheteroaromatic scaffolds, (3,3′-bithianaphthene). As the stereogenic element coincides with the electroactive one, films of impressive chiroptical activity and outstanding enantiodiscrimination properties are obtained. Moreover, chirality manifestations can be finely and reversibly tuned by the electric potential, as progressive injection of holes forces the two thianaphthene rings to co-planarize to favor delocalization. Such deformations, revealed by CD spectroelectrochemistry, are elastic and reversible, thus suggesting a breathing system.*

The combination of chirality with electrical conductivity endows organic polyconjugated materials with a variety of attractive features:[1] 1) the ordered spontaneous chain assembly induced by chirality;[2] 2) non-centrosymmetry, a prerequisite for second-order NLO applications;[3,4] 3) the ability to discriminate between enantiomers, which is required in chemical sensors designed for the detection of chiral analytes;[5–7] 4) the ability to act as chiral electrode surfaces for asymmetric redox reactions.[8]

Chirality is usually introduced into the materials by attaching chiral pendants to the electroactive conjugated backbone through suitable linkers[1] and many different chiral substituents have been either chosen from the chiral pool, such as sugars and amino acids, or manmade for dedicated applications. The presence of carbon stereocenters invariably characterizes the chiral substituents. Polyconjugated systems designed according to this strategy manifest significant chirality only in particular aggregation states.[9–12] A limited number of examples are known in which a stereogenic axis is employed, either installed outside the main conjugated chain,[13] with the same function played by the pendants discussed before, or directly inserted into the backbone. Unfortunately, the stereogenic architectures designed so far either interrupt the conjugative sequence or the corresponding materials are employed as racemates.[14,15]

We have therefore designed and synthesized electroactive chiral poly-heterocycles where chirality is not external to the electroactive backbone but inherent to it. These poly-heterocycles are prepared by chemical or electrochemical oxidation of monomers of the general structure **1** (Scheme 1). Importantly, the same conjugated system responsible for the optical and electrochemical properties of these materials is also responsible for molecular chirality, thus implying that the chiroptical and the enantiorecognition properties of the material are strictly correlated to the electrochemical ones.

The molecular design is based on the following rationale: 1) chirality results from an internal torsion in the conjugated backbone (from here the appellative of inherently chiral monomers); 2) a suitably substituted atropisomeric biheteroaromatic scaffold (a bithiophene or a bipyrrole system) is

[*] Prof. F. Sannicolò, S. Arnaboldi, Dr. V. Bonometti, Prof. P. R. Mussini, Dr. M. Panigati
Università di Milano, Dip. di Chimica and C.I.Ma.I.NA
via Golgi 19, 20133 Milano (Italy)
E-mail: francesco.sannicolo@unimi.it
Prof. T. Benincori
Dip. di Scienza e Alta Tecnologia, Università degli Studi dell'Insubria, via Valleggio 11, 22100 Como (Italy)
Dr. R. Cirilli
Dip. del Farmaco, Istituto Superiore di Sanità
Viale Regina Elena, 299, 00161 Roma (Italy)
Prof. L. Dunsch
Center of Spectroelectrochemistry, Dept. of Electrochemistry and Conducting Polymers, Leibniz Institute of Solid State and Materials Research (IFW), Helmholtzstrasse 20, 01171 Dresden (Germany)
Prof. W. Kutner
Inst. of Physical Chemistry, Polish Academy of Sciences
Kasprzaka 44/52 01-224 Warsaw (Poland)
Prof. G. Longhi
Dip. di Medicina Moleculare e Traslazionale, Università degli Studi di Brescia, Viale Europa 11, 25121 Brescia (Italy)
Prof. M. Pierini
Dip. di Chimica e Tecnologie del Farmaco, Università degli Studi di Roma "La Sapienza", P.le Aldo Moro 5, 00185 Roma (Italy)
Dr. S. Rizzo
Ist. di Scienze e Tecnologie Molecolari, Consiglio Nazionale delle Ricerche, via Golgi 19, 20133 Milano (Italy)

[**] We gratefully acknowledge the support of Prof. Sergio Abbate and Dr. Ettore Castiglioni (polymers CD measurements), Dr. Letizia Colella (Organic synthesis), Dr. Mirko Magni and Dr. Ester Giussani (EIS and enantiorecognition tests), Dr. Krzysztof Noworyta (EQCM), Dr. Sergio Menta (Chiral HPLC), Dr. Kinga Haubner (EPR spectroelectro chemistry), and Prof. A. Gennaro and Dr. A. A. Isse (scientific discussions). With the contribution of Fondazione Cariplo, grant no. 2011-0417.

Supporting information for this article is available on the WWW under http://dx.doi.org/10.1002/anie.201309585.

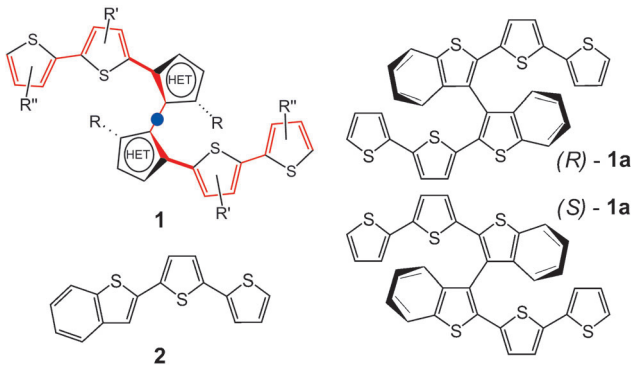

Scheme 1. General structure (**1**) of the monomers. Structures of (*R*)-**1a** and (*S*)-**1a** which are used as monomers in the present work. Structure of **2** (the half subunit of **1a**).

responsible for chain torsion; 3) the stereogenic unit is tailored to conjugatively interconnect the two 2-(5,2′-bithienyl) moieties (red bonds in **1**); 4) a "node" (·)[16] is located on the interannular bond, but distorsion from coplanarity of the two halves should not preclude conjugative interaction. In addition, the three-dimensional (3D) structure of the polyconjugated network is important for amplifying the electro-optical performance of organic semiconductors;[17] 5) the C_2 symmetry of these molecules makes the thiophene α-positions involved in the oxidative coupling homotopic, thus assuring complete regioregularity in the products. Notably, each propagation step (dimerization, trimerization, etc.) invariably results in C_2 symmetric materials.

The first substrates we considered were (*R*)-**1a** and (*S*)-**1a**, in which R′ = R″ = H and R is incorporated into the benzene ring of a 3,3′-bithianaphthene unit. Interestingly, the 3,3′-junction of the internal thiophene units, generally considered a defective connection in polyconjugated systems, does play the essential role of granting electronic communication between the two halves of the molecule. The compound **1a** was selected because racemic (±)-**1a** is easily accessible and we recently proposed its synthesis.[18] Moreover, **1a** rapidly and regularly oligomerizes, and serves as a 3D promoter building block in copolymerization with monomers endowed with key functional properties which do not undergo electropolymerization easily.[19]

The DFT calculations provided an evaluation of the stereochemical properties of **1a**. It appeared that the favored dihedral angle is about 80° (the angle value computed by averaging those found within the two most representative conformations of **1a**, characterized by a relative Boltzmann population of 74% and 26%) and the enantiomerization barrier, related to rotation around the bond connecting the thianaphthene units, is close to 167 kJ mol^{-1}, thus indicating a high configurational stability of the enantiomers even at high temperatures (see the Supporting Information).

The communication between the two thianaphthene units of **1a** through the node was demonstrated by comparing the electronic spectrum and the CV features of the latter with that of 2-[2-(5,2′-bithienyl)]thianaphthene (**2**), which corresponds to half of **1a** (see the Supporting Information).

The resolution of racemic (±)-**1a** was successfully achieved by HPLC on a semipreparative level (Figure 1a). The chiroptical properties of the enantiopure antipodes were determined and the absolute configuration assigned to them by comparing the experimental CD spectra with that calculated for the (*S*)-**1a** enantiomer (Figure 1b; see the Supporting Information).

The potentiodynamic electrooligomerization of (±)-**1a**[18] and that of the enantiomers develops regularly by potential cycling in dichloromethane, resulting in highly stable films of enhanced conjugation with respect to the monomers. They are constituted of oligomers, from the dimer, the largely prevailing one, to the hexamer (Laser Desorption Ionization, LDI), and exhibit charge-trapping features (see the Supporting Information). The electro-oligomerization is also efficient in acetonitrile,[20] while in the 1-butyl-3-methylimidazolium hexafluorophosphate (BMIM)PF_6 ionic liquid (IL) it requires significantly higher monomer concentrations and is much slower. Under these conditions, the oligomerization of enantiopure **1a** was slower than that of the racemate.

Noticeably, in spite of the oligomeric nature of the material, consistent with the low operating monomer concentration, even the dimer of **1a** contains no less than twelve

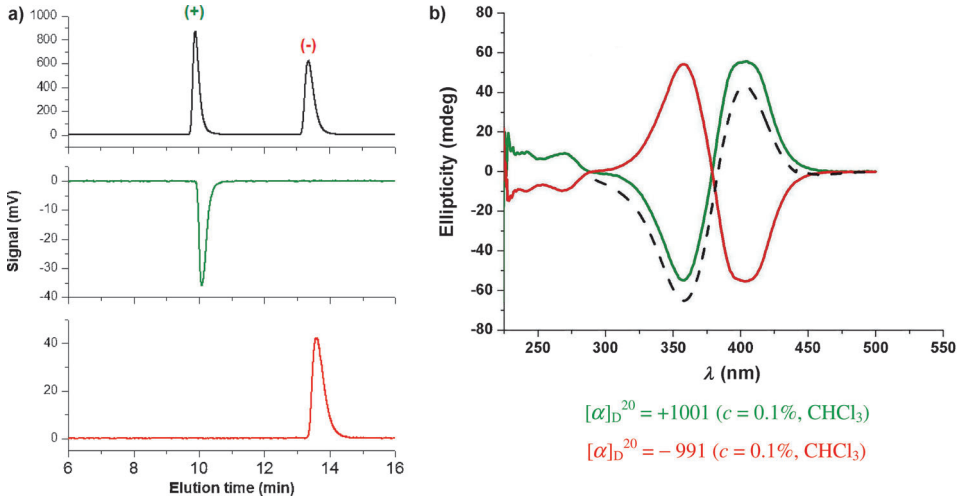

Figure 1. a) Analytical HPLC resolution of (±)-**1a** and purity check of the enantiomers isolated on a semipreparative scale. Column: Chiralpak IB-3 (250×4.6 mm I.D.); eluent: *n*-hexane/CH_2Cl_2/EtOH = 100:5:0.2 (v/v/v); T = 25 °C; (detector UV at λ = 360 nm, detector CD at λ = 360 nm). Black: (±)-**1a** ; green: first eluted enantiomer, (+)-**1a**; red: second eluted enantiomer, (−)-**1a**. b) CD spectra ($CHCl_3$, c = 0.14 mg cm^{-3}) of (*S*)-(+)-**1a** (green) and (*R*)-(−)-**1a** (red). Dotted black curve: calculated CD spectrum for (*S*)-**1a**.

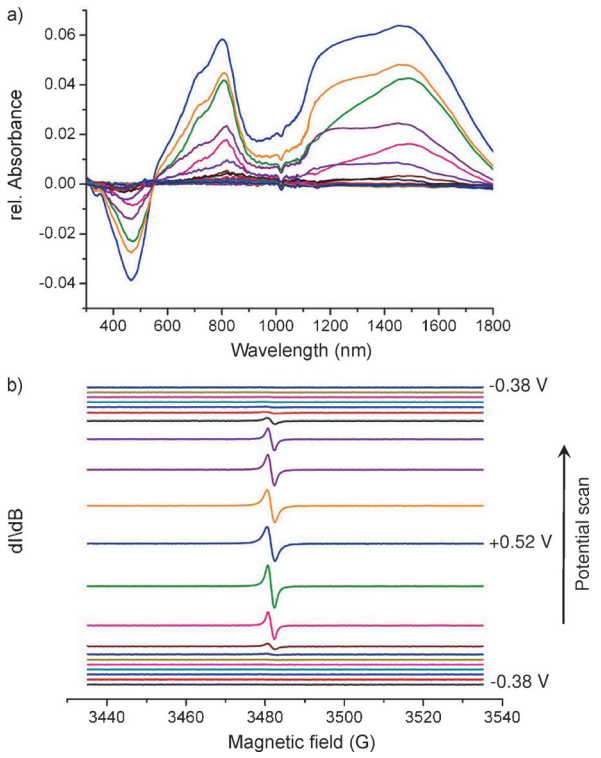

Figure 2. Combined Vis/NIR (a) and ESR (b) data collected by in situ spectroelectrochemistry spectra on a (±)-**1a** film deposited on a Pt electrode grid during a slow CV cycle (5 mVs^{-1}). Potentials are referred to the $Fc^+|Fc$ couple. Vis/NIR and ESR spectra, correlated by colors, are reported at constant potential intervals. Vis/NIR traces are plotted as differences with respect to the spectrum of the neutral film. ESR g factor: 2.0020.

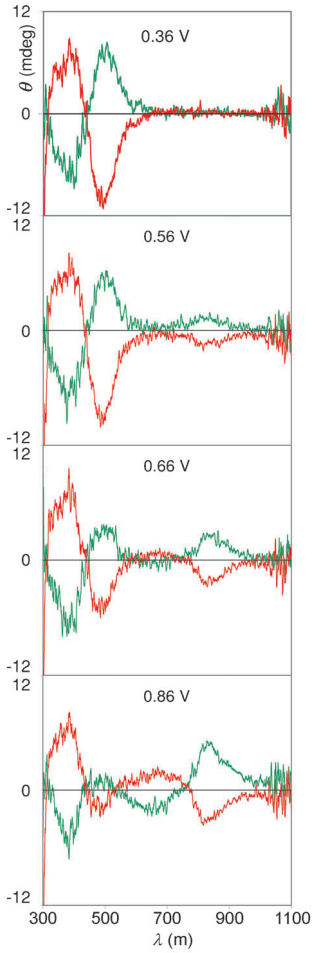

Figure 3. CD spectra of films of oligo-(*R*)-(−)-**1a** (red) and oligo-(*S*)-(+)-**1a** (green) on an ITO electrode during an anodic cycle in 0.1 M (TBA)PF_6 in acetonitrile. Potentials are referenced to the $Fc^+|Fc$ couple.

thiophene units, which is sufficient to endow the material with conducting properties.[20,21]

UV spectroelectrochemistry experiments (Figure 2a) demonstrate that the stepwise increase of the anodic potential produces a strong decrease in intensity of the absorption band at $\lambda \approx 480$ nm with the simultaneous appearance of two new bands at $\lambda \approx 800$ and ≈ 1150 nm, which are attributable to the more conjugated polaronic and bipolaronic states, respectively. Accordingly, parallel in situ ESR spectroelectrochemistry experiments show (Figure 2b) the progressive formation of a radical state with the maximum density signal at 0.52 V vs. $Fc^+|Fc$. This behavior was successfully reproduced by calculations on two of the most representative conformations of **1a** (see the Supporting Information).

Both the first electro-oxidation and the first electro-reduction process of oligo-**1a** are reversible, even though some electroactivity is lost after repeated slow cathodic scans. The most interesting features of these materials are related to their pseudoscalar properties, namely the chiroptical activity and the enantioselection ability.

The CD spectra of the films in the neutral state demonstrate that chirality and its CD sign are directly transferred from monomer to oligomers (spectra for 0.36 V in Figure 3). The bisignate spectra of the oligomers display curves which are very similar to those of the original monomers (Figure 1b), with ellipticity maxima strongly shifted toward higher wavelengths, in accordance with the increased conjugation gained with oligomerization.

The changes in the CD spectrum of the chiral films resulting from potential variations provide insight into the electronic state of the material. For these experiments, a quartz cuvette was adapted to serve as the three-electrode cell fitted with an indium tin oxide (ITO) working electrode coated by either a film of electrodeposited oligo-(*S*)-(+)-**1a** or oligo-(*R*)-(−)-**1a**, together with a saturated calomel electrode (SCE) and a Pt wire as the reference and counter electrode, respectively. The CD spectra of the films, recorded at different applied potentials, parallel the UV spectra: they progressively decrease in their lower energy component with the potential increase, while new signals grow in at higher wavelengths, as expected on the basis of the UV data. Interestingly, the ellipticity of the new signals is considerably lower than the original one, thus indicating a decrease in the chirality in the oxidized state. Injection of holes would force the two thianaphthene rings to co-planarize to gain electronic conjugation with some loss in the stereogenic efficacy of the atropisomeric core.

This suggestion is supported by the DFT calculations, indicating that a remarkable dihedral angle decrease from 80° to 71° is caused by abstraction of one electron from **1a** (see the Supporting Information). The two interconnected heteroaromatic units, however, cannot become coplanar in the heavily doped state, otherwise enantiomeric purity would be lost, whereas the signal is fully recovered when the oligomer is reduced back to its neutral state. This process was perfectly reversible and indefinitely repeatable.

As a preliminary test for the enantiorecognition ability of the enantiomeric films, the CV curves of commercial (*S*)-(−)- and (*R*)-(+)-*N*,*N*-dimethyl-1-ferrocenylethylamine, (*S*)-(**3**) and (*R*)-(**3**), used as chiral probes, were recorded on a bare

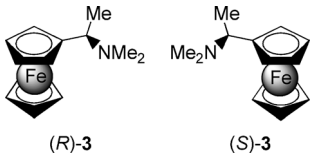

(*R*)-**3** (*S*)-**3**

Au electrode and on two gold electrodes, one coated with the film of oligo-(*R*)-(−)-**1a** and the other with that of oligo-(*S*)-(+)-**1a**.

A prerequisite for this study is the preparation of electrode surfaces which are fully reproducible in size, shape, morphology, and thickness. These requirements were fulfilled by using screen-printed electrodes (an Au working electrode, bare or film-coated, a Pt counter electrode, an Ag pseudoreference electrode) and the (BMIM)PF_6 as the working medium.

On the bare Au electrode, a typical diffusion-controlled reversible peak couple is observed for both (*S*)-(**3**) and (*R*)-(**3**). Both CV curves show peaks at formal potential $E^{\circ\prime} = -0.01$ V vs. $Fc^+|Fc$ with about 60 mV half-peak width and approximately a 60 mV anodic-to-cathodic peak potential separation, as expected for a reversible one-electron transfer.

On the oligomer-film-coated electrodes (36 oligomerization potential cycles for 12 mM **1a** at 50 mV s^{-1}) the enantiomorphic oligo-(*R*)-(−)-**1a** and oligo-(*S*)-(+)-**1a** films display an outstanding, perfectly specular enantiodiscrimination ability towards the (*R*)-**3** and (*S*)-**3** probes, with a formal potential difference of about 0.10 V between the two enantiomers (Figure 4):

1) on the oligo-(*S*)-(+)-**1a** film coated electrode, the formal redox potentials are +0.07 and +0.17 V vs. $Fc^+|Fc$ for (*S*)-**3** and (*R*)-**3**, respectively (Figure 4a);
2) on the oligo-(*R*)-(−)-**1a** film coated electrode, the formal redox potentials are +0.07 and +0.17 V vs. $Fc^+|Fc$ for (*R*)-**3** and (*S*)-**3**, respectively (Figure 4b).
3) separation of formal potentials is even larger for racemic (±)-**3** (Figure 4c).

Considering that the formal potential of the probes falls in the potential range in which the film is neutral, the electron-transfer process must take place at the interphase between the metal electrode and the probe molecule, within the chiral film. Actually the redox peaks remain fully reversible on the film-coated electrode, albeit shifted to more positive potentials, and the potential difference between forward and backward peaks significantly decreases. Both these features point to an electron-transfer process within the chiral film. This information implies that the latter differently affects, through diastereomeric interactions, the energetics of the electron-transfer process in both thermodynamic and kinetic terms.

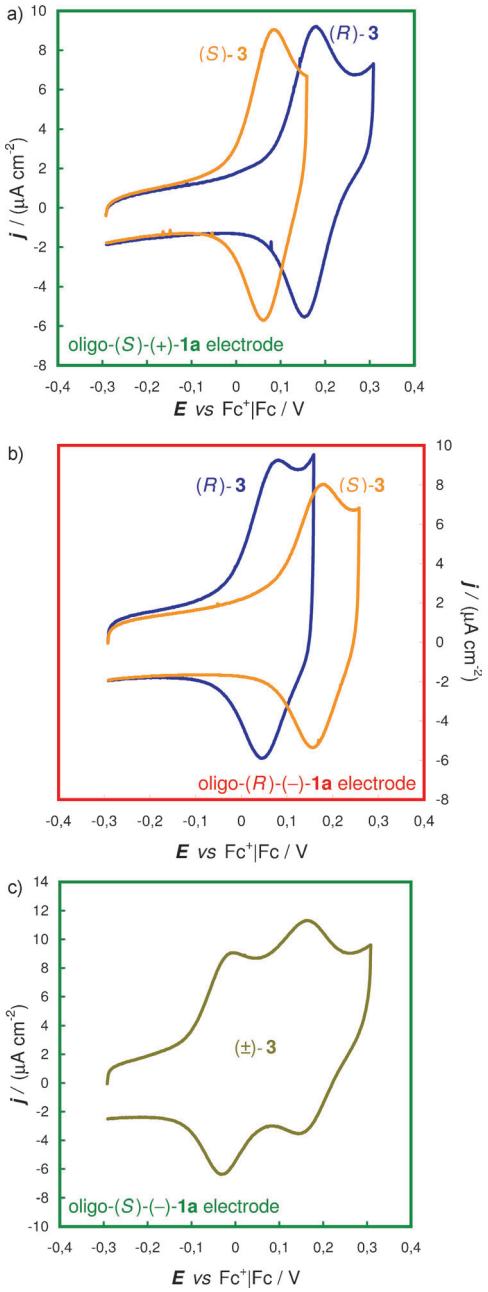

Figure 4. a) Enantiorecognition CV tests for the oligo-(*S*)-(+)-**1a** (a) and oligo-(*R*)-(−)-**1a** (b) film coated Au electrodes with (*R*)-**3** and (*S*)-**3** chiral redox probes (8 mM). c) Data also shown for the oligo-(*S*)-(−)-**1a** film coated Au electrode with the (±)-**3** racemic redox probe. Potential scan rate: 50 mV s^{-1}.

Moreover, we verified that the impressive enantiodiscrimination effect exerted by the chirotopic electrode surface towards the antipodes of the probes is reversible. In fact, the

probe-free film can be easily recovered by performing a few CV cycles around the first oxidation potential in a blank solution. This recovery enabled us to perform multiple subsequent enantiorecognition tests, alternating the *S* and *R* probes, on both the enantiomorphic surfaces starting from either enantiomer.

In conclusion, an innovative strategy is devised for designing inherently chiral electroactive poly-heterocycles exhibiting outstanding chiroptical properties. Moreover, electrodes functionalized with the same films display outstanding enantioselection properties, thus promising stereoselective electroanalysis and electrocatalysis applications. The CD spectra of the films undergo reversible potential-driven variations following the dihedral angle modifications undergone by the atropisomeric backbone, thus suggesting to us the figure of a "breathing" system.

Received: November 4, 2013
Published online: February 5, 2014

Keywords: chirality · circular dichroism · electrochemistry · heterocycles · oligomerization

[1] For a recent complete review on chiral conducting polymers see: L. A. P. Kane-Maguire, G. G. Wallace, *Chem. Soc. Rev.* **2010**, *39*, 2545 – 2576, and references therein.
[2] A. S. Ribeiro, L. M. O. Ribeiro, S. M. M. Leite, J. Da Silva, Jr., J. C. Ramos, M. Navarro, J. Tonholo, *Polymer* **2006**, *47*, 8430 – 8435.
[3] D. Cornelis, E. Franz, I. Asselberghs, K. Clays, T. Verbiest, G. Koeckelberghs, *J. Am. Chem. Soc.* **2011**, *133*, 1317 – 1327.
[4] T. Verbiest, S. Sioncke, G. Koeckelberghs, C. Samin, A. Persoons, E. Botek, J. M. André, B. Campagne, *Chem. Phys. Lett.* **2005**, *404*, 112 – 115.
[5] L. Torsi, G. M. Farinola, F. Marinelli, M. C. Tanese, O. H. Omar, L. Valli, F. Babudri, F. Palmisano, P. G. Zambonin, F. Naso, *Nat. Mater.* **2008**, *7*, 412 – 417.
[6] B. J. De Lacy Costello, N. M. Ratcliffe, P. S. Sivanand, *Synth. Met.* **2003**, *139*, 43 – 55.
[7] M. Lemaire, D. Delabouglise, R. Garreau, A. Guy, J. Roncali, *J. Chem. Soc. Chem. Commun.* **1988**, 658 – 661.
[8] M. Schwientek, S. Pleus, C. H. Hamann, *J. Electroanal. Chem.* **1999**, *461*, 94 – 101.
[9] B. M. W. Langeveld-Voss, R. A. J. Janssen, E. W. Meijer, *J. Mol. Struct.* **2000**, *521*, 285 – 301.
[10] B. M. W. Langeveld-Voss, M. P. T. Christiaans, R. A. J. Janssen, E. W. Meijer, *Macromolecules* **1998**, *31*, 6702 – 6704.
[11] B. M. W. Langeveld-Voss, R. J. M. Waterval, R. A. J. Janssen, E. W. Meijer, *Macromolecules* **1999**, *32*, 227 – 230.
[12] H. Goto, Y. S. Yeong, K. Akagi, *Macromol. Rapid Commun.* **2005**, *26*, 164 – 167.
[13] G. Fukuhara, Y. Inoue, *Chem. Eur. J.* **2010**, *16*, 7859 – 7864.
[14] C. L. Schenck, J. M. Nadeau, *Tetrahedron* **2010**, *66*, 462 – 466.
[15] M. J. Marsella, I. T. Kim, F. Tam, *J. Am. Chem. Soc.* **2000**, *122*, 974 – 975.
[16] T. Benincori, V. Bonometti, F. De Angelis, L. Falciola, M. Muccini, P. R. Mussini, T. Pilati, G. Rampinini, S. Rizzo, F. Sannicolò, S. Toffanin, *Chem. Eur. J.* **2010**, *16*, 9086 – 9098.
[17] J. Roncali, P. Leriche, A. Cravino, *Adv. Mater.* **2007**, *19*, 2045 – 2060.
[18] F. Sannicolò, S. Rizzo, T. Benincori, W. Kutner, K. Noworyta, J. W. Sobczak, V. Bonometti, L. Falciola, P. R. Mussini, M. Pierini, *Electrochim. Acta* **2010**, *55*, 8352 – 8364.
[19] A. Pietrzyk, W. Kutner, R. Chitta, M. E. Zandler, F. D'Souza, F. Sannicolò, P. R. Mussini, *Anal. Chem.* **2009**, *81*, 10061 – 10070.
[20] J. Heinze, B. A. Frontana-Uribe, S. Ludwigs, *Chem. Rev.* **2010**, *110*, 4724 – 4771.
[21] *Handbook of Thiophene-Based Materials: Applications in Organic Electronics and Photonics*, *Vol. 1* (Eds.: I. F. Perepichka. D. F. Perepichka), Wiley, Chichester, **2009**, p. 376.

